BIOLOGY OF REPRODUCTION **80,** 665–673 (2009)
Published online before print 23 December 2008.
DOI 10.1095/biolreprod.108.073833

Chlamydia Infection Causes Loss of Pacemaker Cells and Inhibits Oocyte Transport in the Mouse Oviduct[1]

Rose Ellen Dixon,[3] Sung Jin Hwang,[3] Grant W. Hennig,[3] Kyle H. Ramsey,[4] Justin H. Schripsema,[4] Kenton M. Sanders,[3] and Sean M. Ward[2,3]

Department of Physiology and Cell Biology,[3] University of Nevada School of Medicine, Reno, Nevada
Department of Microbiology and Immunology,[4] Chicago College of Osteopathic Medicine, Midwestern University, Downers Grove, Illinois

ABSTRACT

***Chlamydia trachomatis* is a common sexually transmitted bacterial infection that results in health care costs in the United States that exceed $2 billion per year. *Chlamydia* infections cause damage to the oviducts, resulting in ectopic pregnancy and tubal factor infertility, but the reasons for defective oviduct function are poorly understood. We have investigated the role of oviduct contractions in egg transport and found that underlying electrical pacemaker activity is responsible for oviduct motility and egg transport. Specialized pacemaker cells, referred to as oviduct interstitial cells of Cajal (ICC-OVI), are responsible for pacemaker activity. The ICC-OVI, labeled with antibodies to KIT protein, form a dense network associated with the smooth muscle cells along the entire length of the oviduct. Selective removal of ICC-OVI with KIT-neutralizing antibody resulted in loss of electrical rhythmicity and loss of propulsive contractions of the oviduct. We tested whether infection might adversely affect the ICC-OVI. Mice infected with *Chlamydia muridarum* displayed dilation of oviducts, pyosalpinx, and loss of spontaneous contractile activity. Morphological inspection showed disruption of ICC-OVI networks, and electrophysiological recordings showed loss of intrinsic pacemaker activity without change in basal smooth muscle membrane potential. *Chlamydia* infection also was associated with upregulation of NOS2 (iNOS) and PTGS2 (COX II) in leukocytes. Loss of ICC-OVI and pacemaker activity causes oviduct pseudo-obstruction and loss of propulsive contractions for oocytes. This, accompanied by retention of oviduct secretions, may contribute to the development of tubal factor infertility.**

fallopian tubes, female reproductive tract, interstitial cells, oviduct, ovum pickup/transport

INTRODUCTION

Chlamydia trachomatis is the most common bacterial sexually transmitted disease, presenting an enormous public health challenge worldwide. The World Health Organization estimates that 92 million new cases of *Chlamydia* occurred globally in 1999 [1], and in the United States, 3 million new cases are estimated to occur annually, with the highest incidence in young adults (15 to 25 yr), lower socioeconomic groups, and large urban populations [2]. The health costs of *Chlamydia* infections in the United States are reported to be as high as $2 billion annually [3]. The burden of disease in the developing world is even more significant, with more than two thirds of new *Chlamydia* infections occurring in these regions [4].

Chlamydia is often referred to as "the silent epidemic," because infections are asymptomatic in 70%–75% of women, and consequently often go undiagnosed and untreated [1]. Persistent infection and reinfection after initial clearance is a common feature of *Chlamydia*, often resulting in development of chronic disease and tissue damage as a consequence of the host inflammatory immune response [5]. Thus, women are at high risk of developing severe health problems, including urethritis, cervicitis, and chronic pelvic pain [6]. If untreated, more serious complications, including pelvic inflammatory disease, ectopic pregnancy, and tubal factor infertility (TFI), occur [6]. According to a 2007 World Health Organization report, 10%–40% of women with untreated *Chlamydia* will develop pelvic inflammatory disease [6]. Postinfection damage of the fallopian tubes is estimated to be responsible for 30%–40% of female infertility [6]. However, the biological basis of acute and chronic oviduct inflammation is poorly understood [7].

Little is known about the factors leading to ectopic pregnancies and TFI. Oviduct smooth muscle (myosalpinx) contractions, ciliary beating, and epithelial secretions are thought to provide the propulsive force and lubrication necessary to transport oocytes from the ovary to the uterus [8]. *Chlamydia* infection can lead to stasis of the oviduct, hydrosalpinx (serous fluid-filled oviduct), or pyosalpinx (pus-filled oviduct), and epithelial scarring that can eventually occlude the oviduct lumen.

Interstitial cells of Cajal (ICC) have been reported to populate the oviducts of humans [9–11] and the uterus of both humans and rodent animal models [12, 13]. In the gastrointestinal tract, ICC provide specialized functions, such as pacemaker activity and connectivity with enteric motor neurons [14]. We hypothesize that ICC may be the source of pacemaker activity in the oviduct, producing the electrical activity that drives oviduct contractions and oocyte transport. It is possible that infections cause damage to ICC networks, and this might contribute to oviduct stasis and produce pseudo-obstruction and functional block of oocyte transport and retention of secretions. We used *Chlamydia muridarum* infection as a murine model [4, 15, 16] to determine the impact of *C. muridarum* infection on ICC and oviduct electrical and mechanical behavior. *C. muridarum* infection has been used extensively by others to clarify the host immune response to *Chlamydia* [4]. Persistent or recurrent infections of

[1]Supported by National Institutes of Health grant DK41315 to S.M.W. and K.M.S., and Public Health Service grant AI49354 to K.H.R.
[2]Correspondence: Sean M. Ward, Department of Physiology and Cell Biology, University of Nevada School of Medicine, MS 352, Reno, NV 89557. FAX: 775 784 6903; e-mail: SMWard@medicine.nevada.edu

Received: 30 September 2008.
First decision: 28 October 2008.
Accepted: 4 December 2008.

eISSN: 1259-7268 http://www.biolreprod.org
ISSN: 0006-3363

C. trachomatis in humans lead to infertility, as occurs in mice with induced infections of *C. muridarum* [14]. The genetic profile of *C. muridarum* is similar to human *C. trachomatis*, and for the purposes of this study, acute *C. muridarum* infection provides a reasonable approximation of the acute phase of infection seen in females [4].

MATERIALS AND METHODS

Animal Treatment

BALB/c and C3H/HeN mice between the ages of Postnatal Days 0 (P0) and 70 were used for these studies. Animals were obtained from the Jackson Laboratory (Bar Harbor, ME) or Harlan Sprague-Dawley (Indianapolis, IN). Mice were anesthetized with isoflurane (Baxter, IL) prior to cervical dislocation. The animals were maintained and the experiments performed in accordance with the National Institutes of Health Guide for the Care and Use of Laboratory Animals. The Institutional Animal Use and Care Committees at the University of Nevada and Midwestern University approved all procedures used.

Video Imaging

Oviducts were removed from animals, uncoiled by microdissection from the "proper ligament" of the ovary, and pinned to the base of a Sylgard elastomer-lined (Dow Corning) recording chamber mounted on a Leitz DM-LSM inverted microscope (Leica). The recording chamber was constantly perfused with warmed (37°C), oxygenated Krebs-Ringers buffer (KRB) at a rate of 3 ml min^{-1}, and the oviducts were allowed to equilibrate for 30–60 min before video recording was initiated. Movements of the myosalpinx and transport of the egg cumulus mass were visualized via a 5× objective and a DMK 31AF03 high-resolution fire-wire monochrome camera (30 FPS; The Imaging Source LLC). Images were collected by an iMac computer (Apple) running Astro IIDC software (Aupperle Services and Contracting, Calgary, AB, Canada).

In Vitro Spatiotemporal Mapping

Video analysis was performed on oviduct contractions, egg movements, and luminal particle movements in oviducts obtained from mice after they had received hormones to induce superovulation, as described by the Jackson Laboratory [17]. Briefly, mice received an intraperitoneal injection of 2.5–5 IU of pregnant mare serum gonadotropin (Sigma), followed by the same dose of human chorionic gonadotropin (hCG; Sigma) 46–48 h later. Ovulation occurred approximately 12 h after the hCG injection, after which time a cumulus-oocyte mass (COM) was observed within the oviduct. Spatiotemporal maps (STMaps) of propagating myosalpinx contractions and simultaneous egg or luminal particle movements were constructed from video images as described previously [18]. Briefly, grayscale-coded pixels from each frame of the movie sequence were used to construct a single row and sequential rows, producing STMaps of oviduct diameters. Because of the curved nature of the oviduct wall, instead of vertical pixel columns, a line rotating around a pivot point was used to determine the oviduct diameter at that specific point. Frequency, speed of propagation, and length of oviduct peristaltic waves were measured by placing lines along the white ridges, denoting contraction in the STMaps. A macro developed for this purpose was used to identify the maximal contraction at every point and calculate the slope of the least-square regression line of minimum diameter points during each contraction. The slope of this line represents the average speed of propagation of the contraction. Statistical analysis was performed by applying three sets of ANOVAs to each independent measurement.

The movement of luminal particles (<25 μm), most likely cellular debris, was evaluated for comparison to oocyte transport to evaluate the consequences of ciliary beating. These images were collected via a higher-power objective (60× to 100× magnification). Images were differentiated to determine rate of particle movements within the oviduct.

Electrophysiological and Isometric Force Measurements

Intracellular microelectrode recordings also were made from the myosalpinx at the 50% point along the length of the intact oviduct (i.e., within the isthmus). Muscles were secured in position with tungsten pins (50/1000-inch diameter) to reduce movement and facilitate intracellular recording. Smooth muscle cells were impaled through the outer serosal layer with glass microelectrodes filled with 3 M KCl and having resistances of 80–120 MΩ. Transmembrane potentials were recorded with a high-impedance electrometer (Axoclamp 2B; Axon Instruments). Data were recorded onto a PC via a Digidata 1322A system and Axoscope 9.2 (Axon Instruments). In some experiments, one end of the myosalpinx was anchored using tungsten pins, and the other end was attached to an isometric force transducer (Gould-Statham UC3; Gould-Statham, Oxnard, CA). Microelectrodes were placed along the segment of the myosalpinx from which isometric force recordings were made so simultaneous measurements of intracellular electrical activity and phasic contractile activity could be performed.

Drugs applied to the oviducts were dissolved in KRB and delivered to the muscle at the desired concentration by constant perfusion. In a series of experiments, single pulses of electric field stimulation (EFS; 3- to 10-ms duration), were delivered from a square wave pulse generator (Grass S48; Grass Medical Instruments) via parallel platinum electrodes placed on either side of the oviduct.

Immunohistochemistry

Oviducts were fixed in acetone (10 min at 4°C) or paraformaldehyde (4% w/v in 0.1 M PBS for 30 min at 4°C). After fixation, the tissues were washed for 1 h (acetone fixed) or 24 h (paraformaldehyde solution fixed) in PBS (0.01 M, pH 7.2) and incubated with bovine serum albumin (1% w/v; Sigma Chemical Co. St. Louis, MO) for 1 h at room temperature. For identification of ICC in the oviduct (ICC-OVI), tissues were incubated for 48 h at 4°C with a rat monoclonal antibody raised against KIT protein (ACK2; eBiosciences) at a concentration of 5 μg/ml [19, 20] in 0.01 M PBS containing 0.5% Triton-X 100 (Sigma Chemical). Immunoreactivity was detected using Alexa Fluor 488 goat anti-rat secondary antibody (1:1000 in PBS, 1 h, room temperature; Invitrogen). Before mounting, oviducts were thoroughly washed overnight in 0.01 M PBS to remove excess secondary antibody. The presence of NOS2-immunopositive cells in infected and uninfected C3H/HeN oviducts was assessed using a rabbit polyclonal antibody raised against mouse NOS2 protein (5 μg ml^{-1}; N32030; Transduction Labs). Primary and secondary antibodies were applied in the same manner described above for ACK2, except an Alexa Fluor 488 goat anti-rabbit secondary was used for NOS2. Control experiments were performed in the absence of primary or secondary antibodies. Mounted specimens were examined using a Zeiss LSM 510 Meta confocal microscope (Carl Zeiss). Confocal micrographs of whole mounts were digital composites of the *Z*-series of scans of 1-μm optical sections through the tissue depth. Final images were constructed and montages assembled using Zeiss LSM 5 Image Examiner and Adobe Photoshop CS5 software.

C. muridarum *Infection*

Chlamydia muridarum was grown in HeLa 229 cells as described previously [21, 22]. After progesterone pretreatment, C3H/HeN were inoculated intravaginally with 100–200 median infective dose (5×10^3 to 10×10^3 infectious units) of *C. muridarum* (MoPn), as described previously [16]. Mice were killed 14 days after infection (9–10 wk old), and oviducts were removed for electrophysiology, immunohistochemistry, or molecular/protein analysis. Age- and strain-matched mice were used as uninfected controls.

Organ Culture

Oviducts from BALB/c neonates were cultured for 5 days with or without ACK2 (5 μg/ml; a KIT-neutralizing antibody), as described previously [19, 23]. Electrophysiological and immunohistochemical experiments were performed on the cultured oviducts. Oviducts were isolated from P0 animals and pinned to the base of a sterile tissue culture chamber lined with Sylgard elastomer. Tissues were washed four times with KRB and placed in M199 media (Sigma Chemical) supplemented with penicillin (200 U/ml), streptomycin (200 μg/ml), amphotericin B (0.5 μg/ml), and L-glutamine (2 mM), washed another four times, and incubated at 37°C (90% humidity and 95% O_2-5% CO_2) for up to 7 days, with the culture media being changed every second day. Some tissues were incubated in M199 media containing ACK2 antibody (5 μg/ml). Nonimmune serum was added to culture chambers containing control tissues. For experiments using lipopolysaccharide (LPS) and NOS2 inhibitor (1400W), adult BALB/c oviducts were cultured for up to 1 wk with either LPS (10 μg/ml) in M199 media or LPS (10 μg/ml) and 1400W (1 μM). Control oviducts were cultured for 1 wk in M199 media alone.

Total RNA Isolation and RT-PCR

Total RNA was extracted from oviduct and proximal colon tissues using TRIZOL (Life Technologies, Gaithersburg, MD). The manufacturers' instructions were followed, including the use of polyinosinic acid (20 μg) as an RNA

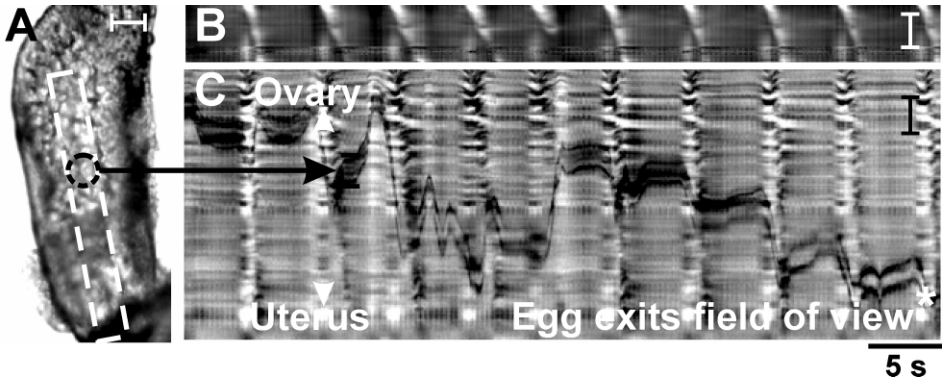

FIG. 1. Propagating myosalpinx contractions propel oocytes toward the uterus. Video analysis and STMaps of myosalpinx contractions and egg movements. **A**) A single video image of an oviduct containing a COM (black dotted circle denotes position of the oocyte in the COM in this frame). Propagating contractions caused indentations in the outer edges of the oviduct, and changes in the edge are summarized in a STMap in **B**. The white diagonal bands in **B** indicate the propagating contractions of the oviduct wall. Propagating contractions caused progression of the oocyte along the lumen of the oviduct. The STMap in **C** tracks oocyte movement as a function of time through the luminal region denoted by the white box in **A**. Parallel black lines in **C** trace the position of the top and bottom edges of the oocyte in the STMap of average intensity. The 5-sec (labeled 5 s) time scale shown below **C** applies for both STMaps **B** and **C**. Bars = 100 μm (**A** and **C**) and 500 μm (**B**).

carrier. First-strand cDNA was prepared from the RNA using Superscript II reverse transcriptase (Life Technologies, Rockville, MD). Total RNA (1 μg) was reverse transcribed with 200 units of reverse transcriptase in a 20-μl reaction containing 25 ng of oligo(dT) primer, dinucleotide triphospates (each at 500 μM), 75 mM KCl, 3 mM $MgCl_2$, 10 mM dithiothreitol, and 50 mM Tris·HCl (pH 8.3). Gene-specific oligonucleotide primers were designed and synthesized for RT-PCR. The PCR reaction was performed using the GeneAmp PCR system 2700 (Applied Biosystems, Foster City, CA) and using 12.5 μl of 2× AmpliTaq Gold PCR Master Mix (Applied Biosystems), 1 μl of the synthesized cDNA, and 10 pM primers in a 25-μl reaction volume. A two-step PCR method (95°C for 10 min, then 40 cycles of 95°C for 15 sec and 60°C for 1 min) was used. After PCR, 2 μl of the RT-PCR product was analyzed on a 2.0% agarose gel.

Western Blots

Total protein was extracted from infected and uninfected C3H/HeN oviducts. Protein concentration of isolated muscle extracts was determined by the Bradford assay (Bio-Rad, Richmond, CA). A total of 30 μg of protein from each lysate was used for the blot. Proteins were subjected to 10% SDS-PAGE and probed with antibodies against CD117 (KIT, 2B8; eBioscience), PTGS2 (COX II; Cayman Chemical), NOS2 (iNOS; Transduction Labs), GAPDH (Santa Cruz Biotechnology), and cyclophilin B (Abcam Inc.). After washing, the blot membrane was incubated with alkaline phosphatase-conjugated anti-rabbit or anti-mouse immunoglobulin G antibody (Santa Cruz Biotechnology). After another wash, the color development was stopped. The amount of proteins on the blot was analyzed using Quantity One 4.5.1 software (Bio-Rad). Image-J software (National Institutes of Health) was used to calculate the relative densities of protein compared with housekeeper [24]. Control experiments were performed in the absence of primary or secondary antibodies.

Drugs and Solutions

Recording chambers for physiological experiments were perfused with oxygenated KRB containing (in mmol/L): NaCl, 120.35; KCl, 5.9; $NaHCO_3$, 15.5; NaH_2PO_4, 1.2; $MgCl_2$, 1.2; $CaCl_2$, 2.5; and glucose, 11.5. The pH of the KRB was maintained at 7.3–7.4 when bubbled with 97% O_2-3% CO_2 at 37°C ± 0.5°C. After pinning, oviducts were left to equilibrate for at least 1 h before experiments were begun. Tetrodotoxin was used to block propagation of action potentials in nerves (Sigma Chemical) and was dissolved in deionized H_2O before being diluted in KRB to the final concentration of 0.3 μM. The L-type calcium channel antagonist, nicardipine (Sigma Chemical), was used in the video imaging experiments where stated at a final concentration of 1 μM to paralyze the myosalpinx. 1400W (dihydrochloride; Cayman Chemical) was used to inhibit NOS2 and was dissolved in ethanol at a stock concentration of 1 mM before being added to the culture medium at a final concentration of 1 μM. Lipopolysaccharide (from *Escherichia coli* serotype 0111:B4; Sigma Chemical) was dissolved in deionized H_2O at a stock concentration of 1000 μg/ml before being added to the culture medium to achieve a final concentration of 10 μg/ml.

Statistical Analysis

Statistical significance was calculated by Student *t*-test or one-way ANOVA analysis depending on the experimental design. All data are expressed as means ± SEMs. The use of "n" in the results section refers to the number of oviducts in which observations were made, with each oviduct being taken from a different animal. *P* values less than 0.05 were considered statistically significant. Measurement of resting membrane potentials (RMPs), amplitude, half-maximal duration, and frequency were made using Clampfit 9.0 (Axon Instruments). Figures displayed were made from digitized data using Adobe Photoshop CS2 (Adobe) and Corel Draw 12.0 (Corel Corp.).

RESULTS

Ciliary Beating Alone Is Insufficient to Propel Eggs along the Oviduct

Video analysis and spatiotemporal mapping were used to investigate the oviduct motility and movements of individual eggs within the COM (n = 6; Fig. 1, A–C) [18]. STMaps of myosalpinx contractions and egg movements showed that propagating contractions of the myosalpinx propel eggs in a pendular manner along the oviduct, with an ultimate bias toward the uterus. As shown in Figure 2, A–C, STMaps revealed egg movements ceased when myosalpinx contractions were inhibited with nicardipine (1 μM; n = 5), but ciliary beating and movement of small (<25 μm) luminal particles persisted (n = 5; Fig. 2, D–F). These data demonstrate that in vitro ciliary beating alone is insufficient to propel oocytes (approximately 80 μm in diameter within the COM), in contrast to previous studies of surrogate egg mass particles approximately 15 μm in diameter [25]. Propulsive movements of the oviduct did not require nerve input because tetrodotoxin (0.3 μM; n = 6) did not inhibit myosalpinx contractions (Supplemental Fig. S1 available at www.biolreprod.org). These findings demonstrate that intrinsic, "myogenic" mechanisms are responsible for oviduct motility.

Slow Waves Provide the Electrical Basis for Spontaneous Rhythmic Contractions

Intracellular electrophysiological recordings were made to determine the basis for oviduct contractility. Smooth muscle cells had diastolic RMPs averaging −58 ± 1 mV, and rhythmic slow waves averaging 37 ± 3 mV in amplitude with a half-maximal duration of 2.4 ± 0.5 sec occurred at a

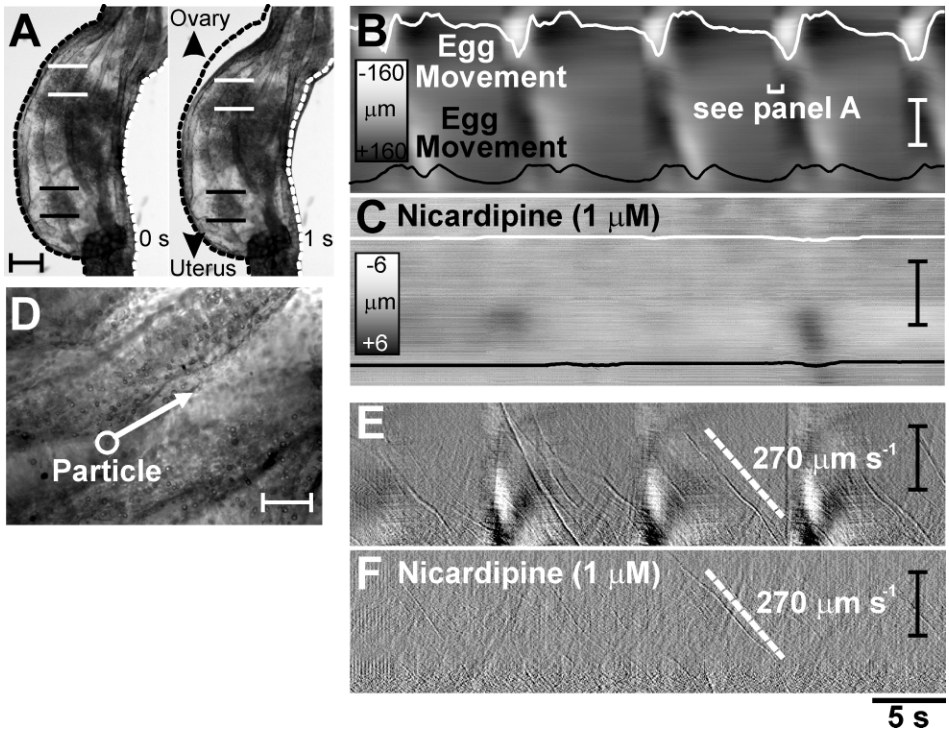

FIG. 2. Egg movement occurs by myosalpinx contractions, not ciliary beating. Illustrated are video analysis and STMaps of myosalpinx contractions, cilia beating, and egg and luminal particle movements before and after nicardipine. **A**) Images of the changes in oviduct diameter (dotted outline) 1 sec (labeled 1 s) apart during a propagating contraction. The regularity of these contractions and the associated movements of two oocytes (identified in **A** by parallel white and black lines) are traced on the STMap as white and black lines in **B**. During the period of time shown, movement was pendular, with little forward progress. Nicardipine (1 μM) blocked the propagating contractions and egg movement (**C**). Scales in **B** and **C** show grayscale representation of diameter. **D**) A high-power image of the epithelium in which particles (<25 μm; white circle-arrow in **D**) that were much smaller than oocytes (70–90 μm) were observed to move along the ciliated epithelium. The differentiated STMap (Δtime = 150 ms) of average intensity (**E**) shows the movement of these particles at ~270 μm sec^{-1} (labeled 270 μm s^{-1}) as thin diagonal streaks (velocity of particle shown as white dotted line) superimposed on regular propagating contractions (thick white areas). Nicardipine (1 μM) blocked regular propagating contractions, but particle movement, most likely via ciliary beating, was unaffected (**F**; ~270 μm sec^{-1}). Time scale shown below **F** applies for **B**, **C**, **E**, and **F**. Bars = 150 μm (**A**); 50 μm (**B** and **D**); and 1 mm (**C**, **E**, and **F**).

frequency of 8.9 ± 1.4 cycles min^{-1}. Slow waves were coupled to phasic contractions that averaged 0.18 ± 0.04 mN and lagged the upstroke of the slow wave by 0.4 ± 0.1 sec (maximum and minimum, 0.75 and 0.17 sec; n = 9; Fig. 3, A and B). Slow waves were insensitive to tetrodotoxin (0.3 μM; n = 6; Supplemental Fig. S1). These data demonstrate that slow-wave depolarizations are the electrical events responsible for phasic contractions of the myosalpinx.

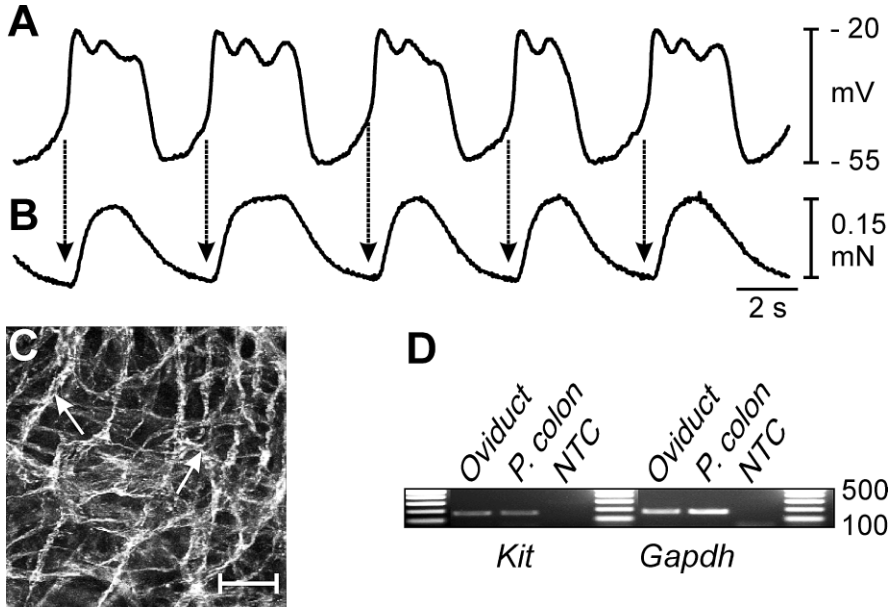

FIG. 3. Spontaneous electrical slow waves are coupled to phasic contractions of the myosalpinx. **A** and **B**) Simultaneous recordings of slow waves and oviduct contractions. Note that each electrical slow wave (**A**) precedes a contraction (**B**) of the myosalpinx (arrows). **C**) Networks of KIT-positive cells (ICC-OVI) were observed in the myosalpinx (arrows). Bar = 50 μm. **D**) RT-PCR confirmed expression of *Kit* in the oviduct, and levels were comparable to expression in muscles of the proximal colon (P. Colon), where ICC are known to be pacemakers [14]. *Gapdh* was used as a housekeeping control, and NTC represents nontemplate control. Units of measurement for data in the gels are bp.

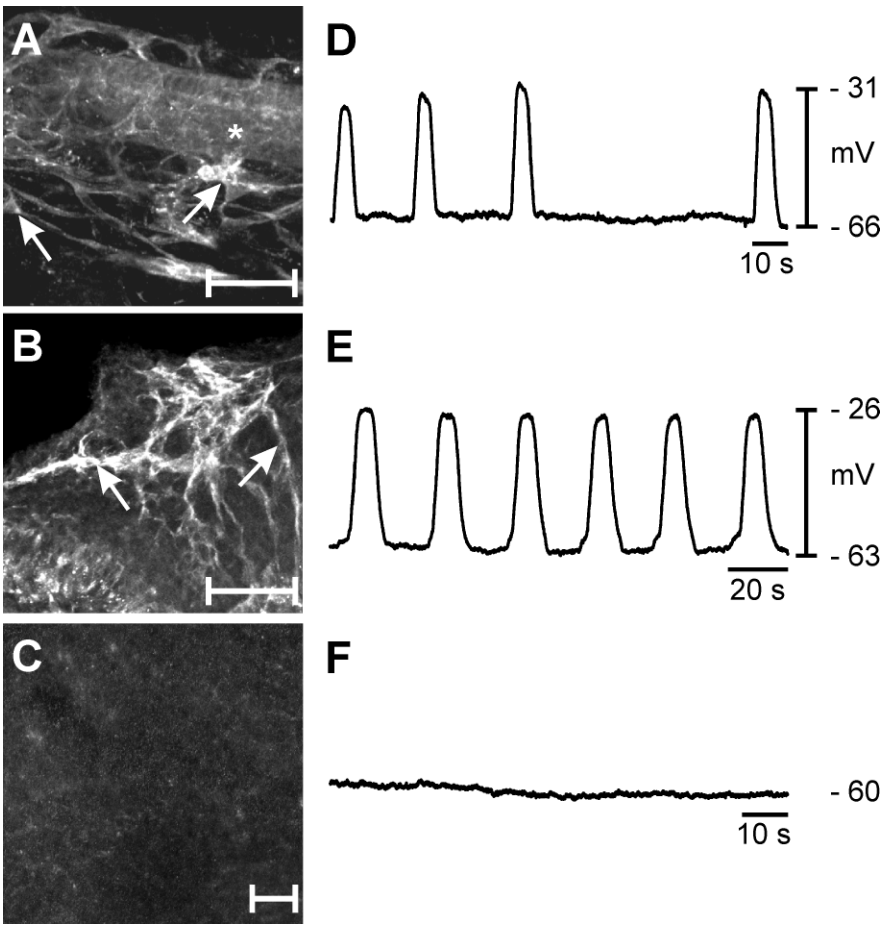

FIG. 4. Loss of ICC-OVI within the myosalpinx leads to a disruption in pacemaker activity. Treatment of P0 oviducts with KIT-neutralizing antibody (ACK2; 5 days) caused loss of ICC-OVI (**C**) compared with P0 oviduct (**A**) and P0 oviduct cultured for 5 days without ACK2 (**B**). The asterisk in **A** indicates the oviduct lumen. Arrows in **A** and **B** identify ICC-OVI cell bodies. Electrical slow waves with irregular frequency were recorded from P0 oviducts (**D**), and this activity became more robust and regular after 5 days in culture (**E**). Pacemaker activity and myosalpinx contractions were lost in oviducts treated with ACK2 for 5 days (**F**). s, seconds. Bars = 50 μm (**A**–**C**).

Dense Networks of KIT-Positive Cells Are Present Along the Oviduct

We investigated the distribution of ICC-like cells in the murine oviduct and whether these cells were involved in pacemaker activity. ICC can be labeled with antibodies for the receptor tyrosine kinase, KIT [19, 20, 26, 27]. Mast cells are also KIT immunopositive and can be visualized in oviduct tissues using ACK2. However, these cells can be distinguished easily from ICC-OVI based on their characteristic scattered distribution and small, rounded morphology [28].

Immunohistochemistry revealed a dense population of KIT-positive cells, with rounded cell bodies and long, slender processes. These cells formed an interconnecting network along the entire length of the oviduct (Fig. 3C and Supplemental Fig. S2). The RT-PCR analysis demonstrated expression of *Kit* that was comparable to gastrointestinal muscles, where ICC represent about 6% of cells in the *tunica muscularis* [29] and serve as stereotypical pacemaker cells (Fig. 3D) [14, 20].

Oviduct ICC Networks and Electrical Rhythmicity Are Dependent on KIT Signaling

We treated oviducts with a neutralizing antibody (ACK2; 5 μg/ml) for KIT to determine 1) the importance of this pathway for maintenance of the ICC phenotype and 2) whether ICC-like cells initiate pacemaker activity in the oviduct [19, 30]. P0 oviducts had RMPs averaging −54 ± 5 mV and generated slow waves 24 ± 4 mV in amplitude with a half-maximal duration of 8.1 ± 2.2 sec and at a frequency of 1.3 ± 0.5 cycles min^{-1} (n = 6; Fig. 4D). ICC-like networks were well established in neonatal oviducts and could be visualized by immunofluorescence (Fig. 4A). ICC networks were still apparent in oviducts in organotypic culture for at least 7 days (Fig. 4B). Pacemaker activity also persisted in cultured oviducts, and more robust activity developed as a function of age, as occurs in vivo. For example, after 5 days in culture, RMPs averaged −52 ± 3 mV, and slow waves 22 ± 4 mV in amplitude with a half-maximal duration of 4.7 ± 0.9 sec occurred at a frequency of 3.2 ± 1.2 cycles min^{-1} (n = 6; Fig. 4E).

ICC networks were disrupted in oviducts cultured with ACK2 (Fig. 4C). Loss of ICC was associated with an absence of pacemaker activity and propulsive contractions in oviducts (n = 5; Fig. 4F), but membrane potentials of smooth muscle cells were unchanged from untreated oviducts (i.e., −56 ± 3 mV; not significantly different from fresh control muscles at P5 or cultured muscles in the absence of ACK2; one-way ANOVA, $P = 0.728$). Thus, loss of slow waves was not due to changes in expression of the ionic conductances responsible for the maintenance of smooth muscle membrane potentials. The term ICC denotes cells with both morphological and functional features [14]. Thus, from our morphological observations (KIT-positive cells) and the link established between ICC-like cells and pacemaker activity in the oviduct, these cells will be referred to subsequently as ICC-OVI.

C. muridarum *Infection Disrupts ICC-OVI Networks and Abolishes Spontaneous Pacemaker Activity*

We next investigated whether inflammatory responses to *Chlamydia* affect ICC-OVI. C3H/HeN mice were intravaginally infected with the obligate intracellular bacterium *C. muridarum* [16, 31, 32]. *Chlamydia muridarum* initiates an

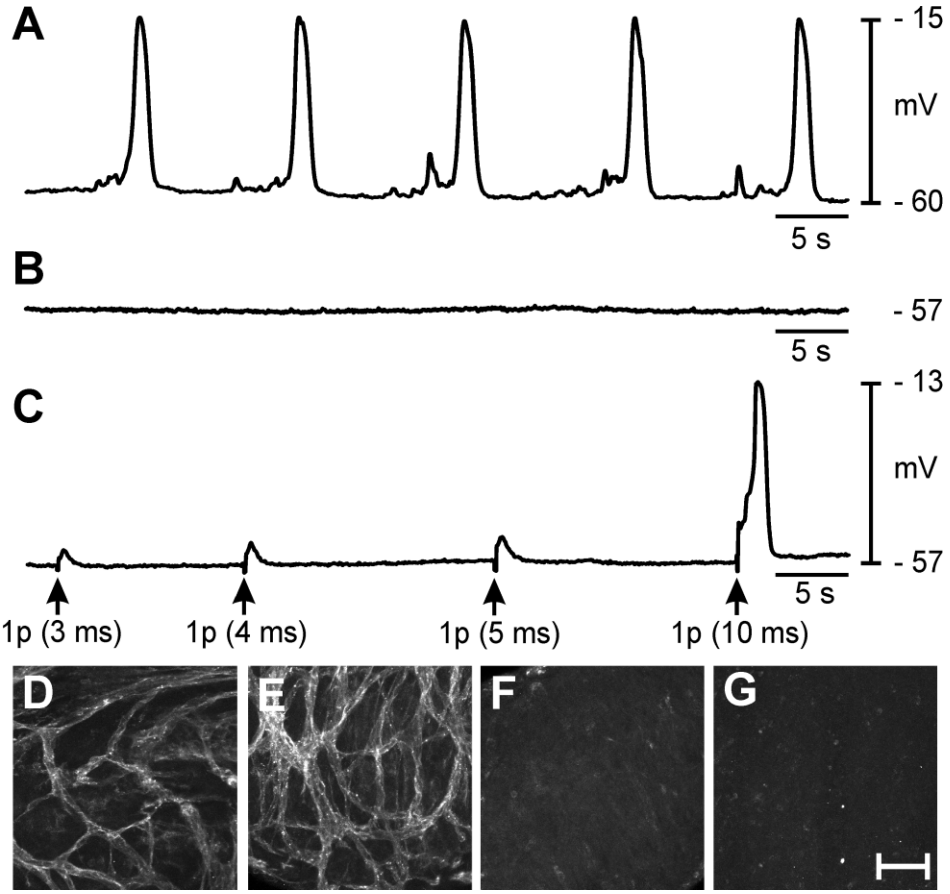

FIG. 5. *Chlamydia muridarum* infection of the female reproductive tract abolishes spontaneous rhythmicity in the oviduct. **A**) Typical slow-wave activity recorded from an adult oviduct. **B**) Absence of pacemaker activity 2 wk after infection with *C. muridarum* is shown. **C**) The myosalpinx of infected oviducts, although not spontaneously active, can be excited by EFS (single pulses [1 p], 3- to 10-ms duration; delivered at arrows). The *C. muridarum* infection causes loss of ICC-OVI along the entire length of the oviduct. (Compare control ICC-OVI networks in **D** [ampulla] and **E** [isthmus] with absence of ICC-OVI in these regions after infection [**F** and **G**]). s, second. Bar = 50 μm (**D**–**G**).

acute inflammatory response in the murine oviduct, as evidenced by pyosalpinx, wall distension, oviduct stasis, and TFI [16, 33]. Fourteen days after a single infusion of *C. muridarum*, mice were killed, and the oviducts were assessed by gross morphological criteria [16], protein analysis, and electrophysiology. Age- and strain-matched mice were used as controls.

Uninfected control mice displayed a dense network of ICC-OVI along the entire length of oviducts (Fig. 5, D and E). Typical electrical slow waves were generated in control oviducts (Fig. 5A). Resting membrane potentials averaged −64 ± 2 mV, and slow waves 46 ± 2 mV in amplitude with a half-maximal duration of 1.2 ± 0.1 sec occurred at a frequency of 6.4 ± 0.8 cycles min^{-1} (n = 6). Oviducts from infected animals were dilated and displayed pyosalpinx. Immunohistochemistry revealed loss of KIT-immunoreactive ICC-OVI along the entire length of infected oviducts in comparison with the dense networks observed in control tissues (Fig. 5, F and G). Spontaneous contractions were absent, and dense luminal secretions made it impossible to visualize the contents of the oviducts or any movements of contents. Resting membrane potentials of smooth muscle cells averaged −56 ± 5 mV (not statistically different from cells in control oviducts; unpaired Student *t* test, $P = 0.148$). In five of six infected oviducts, electrical slow waves were absent (Fig. 5B); however, one infected oviduct displayed small, irregular depolarizations 11 mV in amplitude at 3 cycles min^{-1} (average amplitude and frequency were 1.8 mV and 0.5 cycles min^{-1}, respectively). Oviducts from infected animals were stimulated with EFS. The EFS (>5 ms) evoked smooth muscle depolarizations, demonstrating that the muscle cells were viable and excitable (Fig. 5C). Thus, it appeared that the main functional defect in muscles from infected oviducts was loss of pacemaker activity.

Upregulation of PTGS2 and NOS2 Is Observed in C. muridarum*-Infected Oviducts*

In some smooth muscle tissues, inflammatory responses result in the upregulation of PTGS2 and NOS2 in resident macrophages [34–36]. We investigated whether the loss of ICC-OVI was associated with upregulation of PTGS2 and NOS2 in response to *C. muridarum* infection. Western blot and immunohistochemical analyses were used to determine whether NOS2 expression was affected in *C. muridarum* infection. In agreement with our immunohistochemistry results, Western blot analyses confirmed a decrease in KIT protein expression in infected muscles (Fig. 6, A and B). PTGS2 and NOS2 were not detected in control tissues but were significantly upregulated in infected oviducts (Fig. 6, C–F). Immunohistochemical analysis of infected oviducts revealed that NOS2 was increased in rounded leukocyte-like cells along the oviduct (Fig. 6, G and H).

Induction of NOS2 Alone by LPS Can Abolish ICC-OVI Pacemaker Activity

The NOS2-inducing effects of *C. muridarum* infection were mimicked by inclusion of LPS (Gram negative, 10 μg/ml) in organotypic cultures of adult oviducts. Control experiments were conducted on oviducts cultured for 1–7 days in the absence of LPS or 1400W (n = 9; Fig. 7A). Membrane potential hyperpolarized from −57 ± 8 mV in controls to −67 ± 5 mV in oviducts cultured with LPS for 1–7 days, and pacemaker activity was abolished (i.e., from 10 ± 4 to 0 cycles

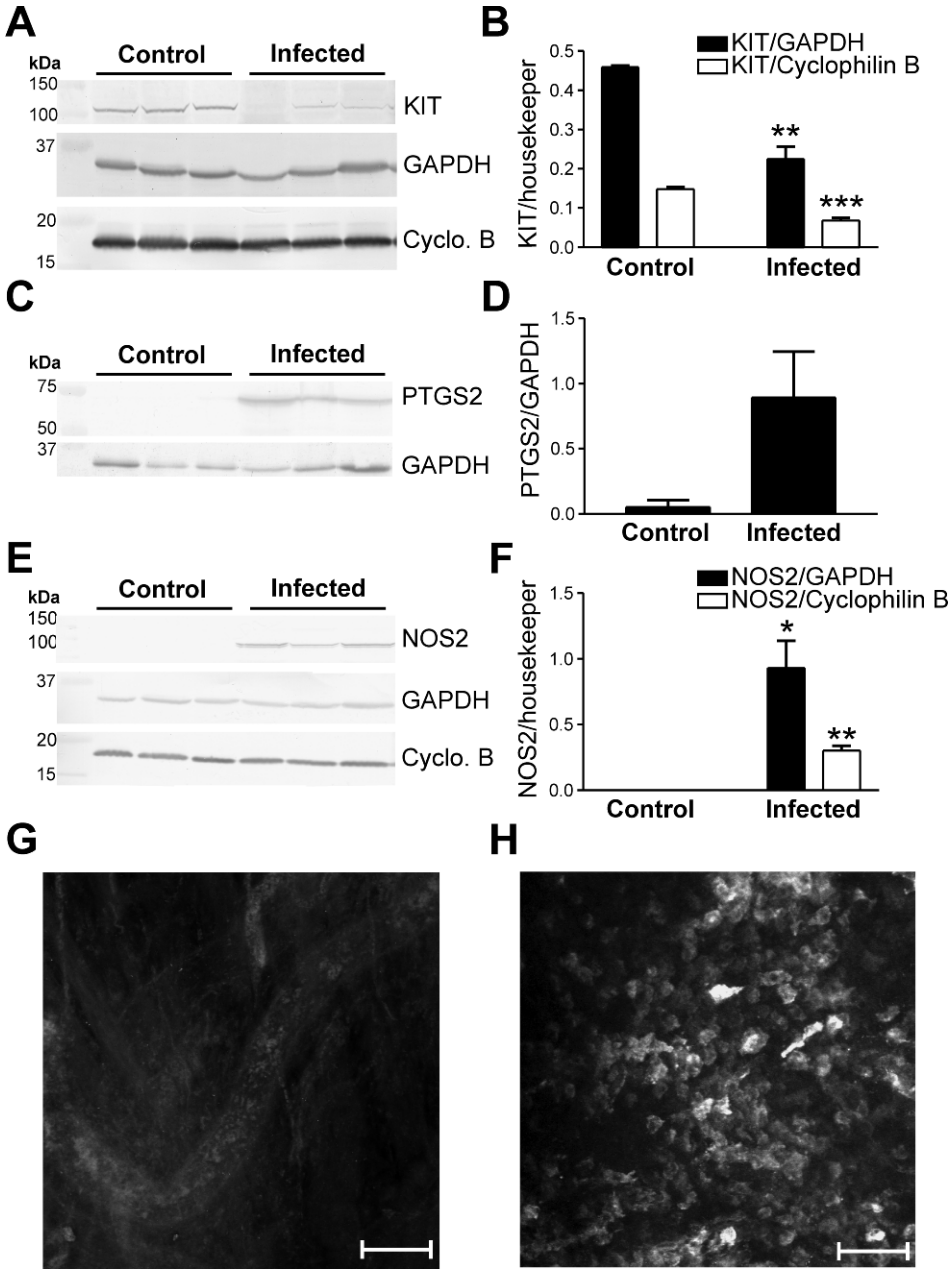

FIG. 6. The inflammatory mediators PTGS2 and NOS2 are upregulated and KIT expression decreases in *C. muridarum*-infected oviducts. **A**) Western blot analysis shows KIT expression is reduced in *C. muridarum*-infected oviducts in comparison with control tissues. Data from three control and three infected animals are tabulated in **B**. Western blots indicate that PTGS2 (**C**) and NOS2 (**E**) were not detected in control oviducts but were upregulated at 2 wk after infection. **D** and **F**) Tabulation of data from three control and three infected animals. **A**, **C**, and **E**) GAPDH and/or cyclophilin B (Cyclo. B) expressions are shown as loading controls and to normalize levels of PTGS2 and NOS2. **G** and **H**) Confocal micrographs showing the lack of NOS2 expression in control tissues and the presence of NOS2-immunopositive cells within the myosalpinx after infection. Statistically significant changes in expression are indicated: $^{*}P < 0.05$, $^{**}P < 0.01$, $^{***}P < 0.001$ (unpaired Student *t*-test). Bars = 100 μm (**G**) and 50 μm (**H**).

min^{-1}; n = 5; $P = 0.046$; Fig. 7, B and C), and the effects on membrane hyperpolarization and pacemaker activity were blocked by addition of the NOS2 inhibitor 1400W (1 μM; n = 5; Fig. 7D). Membrane potential was unchanged at −59 ± 6 mV, and pacemaker activity occurred at a frequency similar to control (10 ± 2 cycles min^{-1}).

DISCUSSION

A long-held dogma in female reproductive physiology has been that ciliary beating provides the chief propulsive force behind egg movement along the oviduct [8, 25, 37]. The results using in vitro STMaps in the present study contradict this concept, because we found that small, 15 to 25 μm particles, possibly cellular debris, were moved in the oviduct by ciliary beating, but eggs are approximately 70–90 μm [38, 39] and are not effectively propelled by ciliary beating. Results we obtained with video imaging experiments demonstrate that spontaneous contractile activity of the myosalpinx is essential for oocyte movement. Blocking smooth muscle contractions with the L-type Ca^{2+} channel antagonist nicardipine caused oviduct stasis and inhibited egg movement. Nicardipine did not affect ciliary beating, as assessed by the movement of small particles along the luminal surface of the duct. Ciliary beating along with oviductal secretions likely provides lubrication of the oviduct and protection of oocytes as they are transported through the oviduct.

Driving the propulsive contractions of the oviduct are electrical slow-wave events that couple in a one-to-one relationship with phasic contractions of the myosalpinx. Slow waves are not initiated by neural inputs, because the activity continued in the presence of tetrodotoxin. Our data suggest that spontaneous slow-wave activity is driven by pacemaker activity provided by ICC-OVI.

This study provides the first evidence that ICC-OVI serve a pacemaker role in the oviduct, and several lines of evidence support this concept. 1) Antibodies for the established biomarker of ICC, KIT [19, 20, 23], labeled a dense population

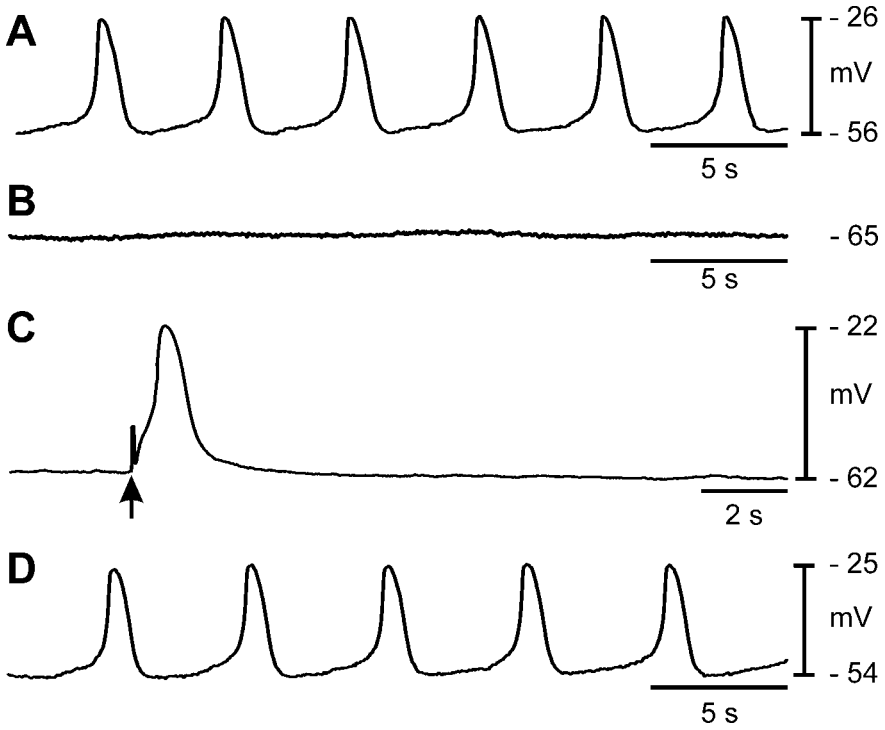

FIG. 7. Oviduct pacemaker activity can be inhibited by LPS. Lipopolysaccharide mimicked the effects of *C. muridarum* infection and abolished pacemaker activity in the oviducts. **A**) Pacemaker activity recorded from control oviducts cultured for 7 days. **B**) Pacemaker activity was absent in an oviduct cultured in the presence of LPS (10 μg/ml). **C**) Slow-wave events could be evoked by EFS in oviducts cultured with LPS (single pulse, 10 ms; arrow). **D**) Cotreatment of cultures with LPS in the presence of the NOS2 inhibitor 1400W (1 μM) protected oviducts from loss of pacemaker activity caused by LPS. s, second.

of ICC-OVI along the entire length of the oviduct. 2) Expression of *Kit* mRNA in the oviduct was comparable to expression in the proximal colon, where ICC generate pacemaker activity [14]. 3) In other types of smooth muscles, KIT signaling is required for development and maintenance of phenotype [23]. Blockade of KIT signaling in oviducts with a neutralizing antibody caused loss of ICC-OVI and abolished pacemaker activity, electrical slow waves, and phasic contractions of the myosalpinx. 4) Finally, pacemaker activity was absent in the oviducts of mice infected with *C. muridarum*, and KIT immunohistochemistry revealed that the likely cause of the loss of pacemaker activity was a depletion of ICC-OVI. Loss of ICC was mirrored by reduced KIT protein in infected oviducts.

A plethora of proinflammatory mediators are released by the host upon infection with *Chlamydia* [4]. The pathway through which *Chlamydia* affects oviduct pathogenesis is extensive and beyond the scope of this study. However, we investigated one phase, the expression of proinflammatory PTGS2 and NOS2, because these two mediators have been implicated previously as host-dependent factors that can damage ICC in inflammation of the gastrointestinal tract [34–36]. Results showed that both PTGS2 and NOS2 were significantly upregulated in infected oviducts, and NOS2 was found to be expressed in leukocytes within the myosalpinx. Thus, it is possible that part of the immune response and disruption of ICC networks could be due to PTGS2 and NOS2.

The significance of NOS2 upregulation was further tested by culturing oviducts in the presence of LPS for 1 wk. Lipopolysaccharide is a derivative of bacterial cell walls. Chlamydial LPS is reported to be 100-fold less potent than other bacterial LPS [4] but, similar to *Chlamydia* infection, LPS caused inhibition of pacemaker activity. Blockade of NOS2 activity with the inhibitor 1400W preserved pacemaker activity. These data suggest that host response upregulation of NOS2, and possibly other proinflammatory mediators, disrupts pacemaker activity, leading to a loss of phasic contractions and egg movement along the oviduct. At the present time, we do not know the specific pathobiology and fate of ICC-OVI during infection and how NO might promote the loss of these cells.

In summary, this study shows that egg propulsion along the oviduct is due to smooth muscle contractions driven by electrical slow waves. ICC-OVI pace the smooth muscle cells of the oviduct to produce propulsive phasic contractions. ICC-OVI are damaged by inflammatory responses to *C. muridarum* infection. Loss of pacemaker activity causes stasis of the oviduct, and the ensuing pseudo-obstruction may lead to blockage and scarring, because secretions and oocytes cannot be cleared. Long-term effects of oviduct stasis may lead to fibrosis and subsequent occlusion, resulting in tubal factor infertility.

ACKNOWLEDGMENTS

The authors wish to express their sincere appreciation to Yulia Bayguinov, Sean P. Clarke, and Paul Scowen for excellent technical assistance.

REFERENCES

1. World Health Organization. Global prevalence and incidence of selected curable sexually transmitted infections overview and estimates. Geneva, Switzerland: WHO; 2001.
2. Adderley-Kelly B, Stephens EM. *Chlamydia*: a major health threat to adolescents and young adults. ABNF J 2005; 16:52–55.
3. Stamm WE. Chlamydia screening: expanding the scope. Ann Intern Med 2004; 141:570–572.
4. Brunham RC, Rey-Ladino J. Immunology of *Chlamydia* infection: implications for a *Chlamydia* trachomatis vaccine. Nat Rev Immunol 2005; 5:149–161.
5. Entrican G, Wattegedera S, Rocchi M, Fleming DC, Kelly RW, Wathne G, Magdalenic V, Howie SE. Induction of inflammatory host immune responses by organisms belonging to the genera *Chlamydia*/*Chlamydophila*. Vet Immunol Immunopathol 2004; 100:179–186.
6. World Health Organization. Global strategy for the prevention and control of sexually transmitted infections: 2006–2015: breaking the chain of transmission. Geneva, Switzerland: WHO; 2007.
7. Leese HJ, Tay JI, Reischl J, Downing SJ. Formation of Fallopian tubal fluid: role of a neglected epithelium. Reproduction 2001; 121:339–346.

8. Croxatto HB. Physiology of gamete and embryo transport through the fallopian tube. Reprod Biomed Online 2002; 4:160–169.
9. Popescu LM, Ciontea SM, Cretoiu D. Interstitial Cajal-like cells in human uterus and fallopian tube. Ann N Y Acad Sci 2007; 1101:139–165.
10. Popescu LM, Ciontea SM, Cretoiu D, Hinescu ME, Radu E, Ionescu N, Ceausu M, Gherghiceanu M, Braga RI, Vasilescu F, Zagrean L, Ardeleanu C. Novel type of interstitial cell (Cajal-like) in human fallopian tube. J Cell Mol Med 2005; 9:479–523.
11. Shafik A, Shafik AA, El Sibai O, Shafik IA. Specialized pacemaking cells in the human Fallopian tube. Mol Hum Reprod 2005; 11:503–505.
12. Duquette RA, Shmygol A, Vaillant C, Mobasheri A, Pope M, Burdyga T, Wray S. Vimentin-positive, c-kit-negative interstitial cells in human and rat uterus: a role in pacemaking? Biol Reprod 2005; 72:276–283.
13. Allix S, Reyes-Gomez E, Aubin-Houzelstein G, Noel D, Tiret L, Panthier JJ, Bernex F. Uterine contractions depend on KIT-positive interstitial cells in the mouse: genetic and pharmacological evidence. Biol Reprod 2008; 79:510–517.
14. Sanders KM. A case for interstitial cells of Cajal as pacemakers and mediators of neurotransmission in the gastrointestinal tract. Gastroenterology 1996; 111:492–515.
15. Read TD, Brunham RC, Shen C, Gill SR, Heidelberg JF, White O, Hickey EK, Peterson J, Utterback T, Berry K, Bass S, Linher K, et al. Genome sequences of *Chlamydia trachomatis* MoPn and *Chlamydia pneumoniae* AR39. Nucleic Acids Res 2000; 28:1397–1406.
16. Shah AA, Schripsema JH, Imtiaz MT, Sigar IM, Kasimos J, Matos PG, Inouye S, Ramsey KH. Histopathologic changes related to fibrotic oviduct occlusion after genital tract infection of mice with *Chlamydia muridarum*. Sex Transm Dis 2005; 32:49–56.
17. Jackson Laboratory. Superovulation technique. Jax Notes, The Jackson Laboratory, Bar Harbor, Maine. 1988;434. World Wide Web (http://jaxmice.jax.org/jaxnotes/archive/434c.html). (September, 2008).
18. Hennig GW, Costa M, Chen BN, Brookes SJ. Quantitative analysis of peristalsis in the guinea-pig small intestine using spatio-temporal maps. J Physiol 1999; 517:575–590.
19. Torihashi S, Ward SM, Nishikawa S, Nishi K, Kobayashi S, Sanders KM. c-kit-dependent development of interstitial cells and electrical activity in the murine gastrointestinal tract. Cell Tissue Res 1995; 280:97–111.
20. Ward SM, Burns AJ, Torihashi S, Sanders KM. Mutation of the proto-oncogene c-kit blocks development of interstitial cells and electrical rhythmicity in murine intestine. J Physiol 1994; 480:91–97.
21. Weiss E, Schramek S, Wilson NN, Newman LW. Deoxyribonucleic acid heterogeneity between human and murine strains of *Chlamydia trachomatis*. Infect Immun 1970; 2:24–28.
22. Caldwell HD, Kromhout J, Schachter J. Purification and partial characterization of the major outer membrane protein of *Chlamydia trachomatis*. Infect Immun 1981; 31:1161–1176.
23. Beckett EA, Ro S, Bayguinov Y, Sanders KM, Ward SM. Kit signaling is essential for development and maintenance of interstitial cells of Cajal and electrical rhythmicity in the embryonic gastrointestinal tract. Dev Dyn 2007; 236:60–72.
24. Rasband WS. ImageJ. Bethesda, MD: National Institutes of Health; 1997.
25. Halbert SA, Becker DR, Szal SE. Ovum transport in the rat oviductal ampulla in the absence of muscle contractility. Biol Reprod 1989; 40: 1131–1136.
26. McCloskey KD, Gurney AM. Kit positive cells in the guinea pig bladder. J Urol 2002; 168:832–836.
27. Burns AJ, Herbert TM, Ward SM, Sanders KM. Interstitial cells of Cajal in the guinea-pig gastrointestinal tract as revealed by c-Kit immunohistochemistry. Cell Tissue Res 1997; 290:11–20.
28. Nissinen MJ, Panula P. Developmental patterns of histamine-like immunoreactivity in the mouse. J Histochem Cytochem 1995; 43:211–227.
29. Ordog T, Redelman D, Horvath VJ, Miller LJ, Horowitz B, Sanders KM. Quantitative analysis by flow cytometry of interstitial cells of Cajal, pacemakers, and mediators of neurotransmission in the gastrointestinal tract. Cytometry A 2004; 62:139–149.
30. Maeda H, Yamagata A, Nishikawa S, Yoshinaga K, Kobayashi S, Nishi K, Nishikawa S. Requirement of c-kit for development of intestinal pacemaker system. Development 1992; 116:369–375.
31. Barron AL, White HJ, Rank RG, Soloff BL, Moses EB. A new animal model for the study of *Chlamydia trachomatis* genital infections: infection of mice with the agent of mouse pneumonitis. J Infect Dis 1981; 143:63–66.
32. Swenson CE, Donegan E, Schachter J. *Chlamydia trachomatis*-induced salpingitis in mice. J Infect Dis 1983; 148:1101–1107.
33. de la Maza LM, Pal S, Khamesipour A, Peterson EM. Intravaginal inoculation of mice with the *Chlamydia trachomatis* mouse pneumonitis biovar results in infertility. Infect Immun 1994; 62:2094–2097.
34. Yanagida H, Sanders KM, Ward SM. Inactivation of inducible nitric oxide synthase protects intestinal pacemaker cells from postoperative damage. J Physiol 2007; 582:755–765.
35. Eskandari MK, Kalff JC, Billiar TR, Lee KK, Bauer AJ. LPS-induced muscularis macrophage nitric oxide suppresses rat jejunal circular muscle activity. Am J Physiol 1999; 277:G478–G486.
36. Kalff JC, Schraut WH, Billiar TR, Simmons RL, Bauer AJ. Role of inducible nitric oxide synthase in postoperative intestinal smooth muscle dysfunction in rodents. Gastroenterology 2000; 118:316–327.
37. Halbert SA, Tam PY, Blandau RJ. Egg transport in the rabbit oviduct: the roles of cilia and muscle. Science 1976; 191:1052–1053.
38. Fitzharris G, Baltz JM. Granulosa cells regulate intracellular pH of the murine growing oocyte via gap junctions: development of independent homeostasis during oocyte growth. Development 2006; 133:591–599.
39. Griffin J, Emery BR, Huang I, Peterson CM, Carrell DT. Comparative analysis of follicle morphology and oocyte diameter in four mammalian species (mouse, hamster, pig, and human). J Exp Clin Assist Reprod 2006; 3:2.